High Frequency Equivalent Circuit Model of the Stator winding in Electrical Machines

Sara Mahdavi, Kay Hameyer

***Abstract* -- Over the years, electrical machinery design strategies have been mainly oriented towards enhancing the output power, power density and torque. However, the effect of machine parameters (geometry, material properties, etc.) on stress and life expectancy has not been considered very often. Since the machines are designed to be as compact as possible, they tend to operate at levels closer to their safety margins. Moreover, the substantial growth in inverter supplying has introduced excessive electrical stress to the winding insulation. This results into earlier partial discharge and bearing currents which may be analyzed by the models that are valid in the high frequency spectrum. This paper introduces a model that can be used to monitor the health-status of the machine's winding by studying these effects. The approach introduced in this paper can localize the mostly stressed parts of the winding fed by inverter by means of measurement and simulation.**

***Index Terms*-- condition monitoring, electrical machine, high frequency model, aging, insulation, life-time estimation**

I. NOMENCLATURE

List of the symbols used in this work is as following:

Symbol	Description
α	Wave travelled distance
C	Capacitance
D	Distance between two neighbor wires in a slot
d_n	Time exponential factor of the n-th voltage wave
ε_0	Permittivity of vacuum
ε_r	Relative permittivity
f	Frequency
K	Capacitance between two wires
l	Length of winding
L	Inductance
λ	Wave length
λ_n	Angular space density of the n-th voltage wave
μ_0	Permeability of vacuum
μ_r	Relative Permeability
ω_n	Angular time frequency of the n-th voltage wave
R	Resistance
ν	Wave velocity
ν_0	Wave velocity in vacuum
R	Resistance
τ	Delay time in pulse arrival
T_R	Rise time of a pulse
u	Voltage wave as a function of time and space

II. INTRODUCTION

Since the invention of electrical machines, engineers have been focusing on optimizing machine geometry and material properties in order to increase efficiency. In addition to the reduction of parasitic effects, high utilization of iron and copper parts has been the main goal of electrical machine design. This trend is economical and in compliance with global energy security restrictions. As a result, today's machines operate at temperatures, voltages, and currents that are closer to their safety margin and are consequently more prone to stress and insulation failure [1]-[3].

Another aspect of particular interest in this work is the prevalent usage of power electronic-inverters as the energy source of motors. Sharp rising edges of inverter voltage pulses tend to propagate as traveling waves in the winding of machines and result into early aging of the insulation[4]-[8]. When studying the response of the machine to the inverter pulses, one should keep in mind, that as long as the source current and voltage frequencies are low, they can travel considerably fast inside the machine windings. Fig. 1 describes this phenomenon: If a voltage wave form is connected to the terminal of the machine coil, it reaches the end of the winding after a delay time τ.

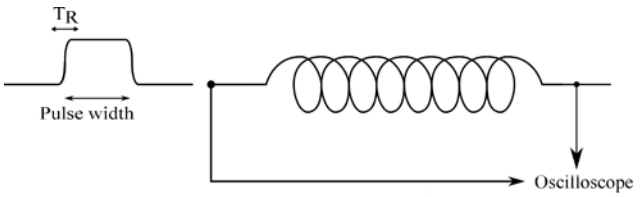

Fig. 1. Measurement configuration: A pulse with a rise time of T_R=0.6 μs and width of 1.1 ms is fed to phase U of a three phase synchronous machine. The voltage is measured at the end of the open circuited terminal of the same phase.

According to (1), if the wave form has low frequency content, it has a large wave length. This is described by the following equation, where f is the frequency, λ is the wavelength and ν is the propagation velocity.

$$f = \lambda \cdot \nu \tag{1}$$

For wire lengths smaller than this wavelength, the delay time is negligible. As a result conventional RL circuits are used for the analysis of normal operation conditions of machines. To understand the reason of early aging of inverter fed machines it is important to use an equivalent circuit model of the machine which can model the winding behavior supplied by steep front pulses. Since the behavior of inverter operated machines cannot be estimated by the conventional RL circuits, some investigation has been performed to model the high frequency behavior of machines including transformer and machine windings [7], [9]-[12]. In the first step of this paper a number of laboratory measurements are performed to observe the high frequency behavior of the winding. Considering the measurement and based on the physics of high frequency wave propagation, a high frequency equivalent circuit is

Sara Mahdavi is a research associate at RWTH Aachen University, 52062 Germany (email: sara.mahdavi@iem.rwth-aachen.de)

Kay Hameyer is the director of Institute of Electrical Machines at RWTH University, 52062 Germany (email: Kay.Hameyer@iem.rwth-aachen.de)

978-1-4673-0142-8/12/$26.00 ©2012 IEEE

developed and introduced. This model includes losses and self inductances as well as physical coupling effects.

III. Measurements

In order to understand the high frequency behavior of an electrical machine, a number of tests has been performed which will be discussed in the following.

A. Case I. Measurement on Phase U

In the first test arrangement a rectangular voltage pulse is connected to phase U of a three phase single layer, synchronous machine shown in Fig.1. This pulse is a surge with a sharp front time of $T_R = 0.6$ µs and a width of 1.1 ms. In terms of frequency content, this pulse is similar to inverter signals, partial discharge pulses and bearing currents [8], [14]- [16].

As this pulse propagates in the winding, it experiences dispersion and attenuation. The input voltage and the voltage signal that reaches the end of the winding are recorded and plotted in Fig. 2.

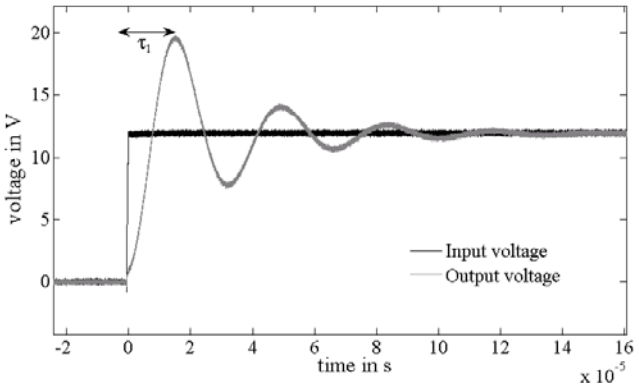

Fig. 2. Measured input (pulse shaped) voltage and output (oscillating) voltage of the test configuration of Fig.1.

The travelled distance α is directly related to the winding length. The relation between the travelled distance α and the delay in pulse arrival time τ_1, gives the effective propagation speed of the pulse inside the machine as in (2).

$$v = \alpha / \tau_1 = 36.42 \text{ m/µs} \quad (2)$$

This value is approximately eight times smaller than the propagation speed in vacuum $v_0 = 300$ m/µs in (3).

$$v_0 = \frac{1}{\sqrt{\varepsilon_0 \bullet \mu_0}} \quad (3)$$

Similar cases have been reported in [17]-[18], where the propagation speed inside the machine's winding is considerably less than v_0. According to (4), the propagation speed in mediums other than vacuum can be reduced depending on the geometric structure and material properties of conductors.

$$v \cong v_0 / \sqrt{C \bullet L} \quad (4)$$

Geometry and material properties both contribute to the values of C and L. Under the assumption that geometry properties are equal, factor $C \cdot L$ in that system can be reduced to $\varepsilon . \mu$ [19]. Knowing that the insulation around the copper wires has a relative permittivity of $\varepsilon_r = 5$, one could substitute (3) in (4) and derive (5). According to (5), one might assume that, iron with a finite relative permeability of $\mu_r \approx 13$ is contributing to pulse propagation.

$$v \cong v_0 / \sqrt{C \cdot L} \cong v_0 / \sqrt{\varepsilon_r \cdot \mu_r} \quad (5)$$

However, some previous studies based on the classical Maxwell equations do not support the idea of reduced permeability for frequency domains below a frequency of 20 MHz [20]. To understand the reason of reduced speed a simple coaxial arrangement is considered as in Fig.3. This arrangement is supposed to help visualize a simplified geometry which resembles a copper wire inside a machine slot. The copper wire resembles the inner conductor of the coaxial cable and the slot iron is its outer conductor, respectively.

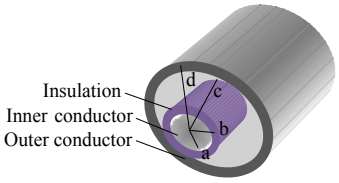

Fig. 3. A simplified slot section which resembles a coaxial cable.

Since the insulation coating on the copper wire is generally much thinner compared to the conductor's dimensions, the capacitance per length between the inner and outer cylinders is derived from (6).

$$C_{coaxial} = 2\pi \varepsilon_0 / \ln \frac{c}{b} \quad (6)$$

If there is no current inside the conductors and only one type of electric insulation is used, the value of inductance per meter would be equal to $L = \varepsilon_r \cdot \mu_r / C_{coaxial}$. When the current flows inside the inner conductor, the outer conductor will also be induced with current. Knowing that the iron is laminated, it is obvious that the outer coaxial conductor of Fig. 3 cannot support the flow of a total axial current. Hence the value of inductance is strongly influenced by the distribution of current inside the iron sheets. This distribution is decided by the frequency content of the conductors, material properties and geometry [20], [23]. For frequency contents within the partial discharge, bearing currents and inverter pulses [8], [14]-[16], the current will close its path through each lamination via the housing or the lamination insulation. This means that unlike the electric field, the flux between stator iron and wire copper (the inner and outer conductors as shown in Fig.3) is not limited to the air gap volume. Hence, $C \cdot L$ factor cannot be simplified to $\varepsilon . \mu$ in machine windings. Therefore, it is not correct to explain the speed reduction by means of reduced permeability in equation (5). The corresponding Maxwell equations are provided in [20], [23].

B. Case II. Measurement on Series Connection of Phase U and phase W

The next test arrangement consists of windings of two phases connected in series, where the pulse voltage is connected to the terminal of winding U and the signal is measured at the end of winding W. The test configuration and test results are illustrated in Fig.4 and Fig.5 respectively.

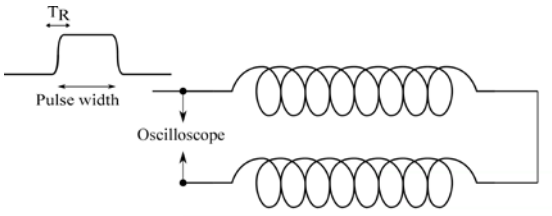

Fig. 4. Measurement configuration: A pulse with a rise time of T_R=0.6 µs and width of 1.1 ms is fed to phase U of a three phase synchronous machine. Phase U is connected to phase W in series. Output voltage is measured at the end of phase W.

The delay time τ_2 in Fig.5 corresponds to the traveling time when two identical phases of the machine are connected in series.

According to transmission line theory [19] and reflection rules, the delay time τ_2 in Fig.4 is supposed to be twice τ_1 of Fig.2. However, a close observation of wave forms proves that the relation between these two numbers is not exactly two ($\tau_2 / \tau_1 = 14.4 / 7.5$). This means the oscillations are dependent on factors that are not fully described in the classical transmission line theory [9], [19]. This is more discussed in more details in terms of factor ω_n in section VIII of this paper, where the oscillation frequency is a not a linear function of propagated length.

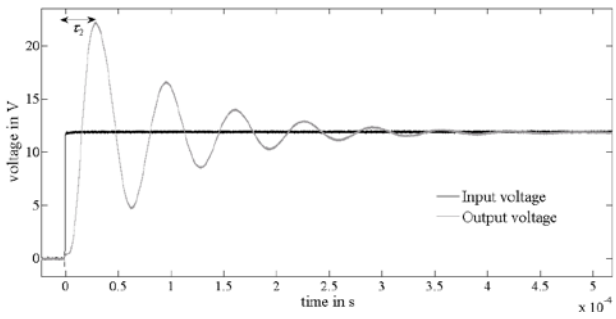

Fig. 5. Measured input (pulse shaped) and output (oscillating) voltage of the test configuration of Fig.4.

C. *Necessity of High Frequency Model Application*

Each phase of the machine has a winding with a length of $l = 274.8$ m. Considering the travelling speed of $v = 36.88$ m/µs, the 0.6 µs front of the input pulse would have a wave length of approximately 22 m inside the slot. This value is comparable to the length of the winding. Hence analyzing it requires the application of distributed models. As mentioned before, the pulse shape is of particular importance since it matches the specifications of partial discharge, bearing currents and inverter impulses [8], [14]-[16]. Consequently this pulse shape can simulate these signals and presents a way of estimating their effect on the life time of the machine.

IV. Equivalent Distributed Circuit

Depending on the harmonic frequency content of the input voltage, the winding can be divided into n sections, each having a length of Δx. The section of the conductors inside the slot is illustrated in Fig.6, where each part of the wire that is surrounded by insulation and iron has losses that can be modeled as $R\Delta x$.

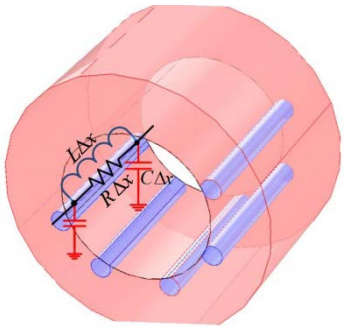

Fig. 6. One section of the high frequency model of a machine with concentrated conductors inside the slot.

More details about the contribution of iron to wave propagation and values of R are presented in [20]. The capacitance to the ground is $C\Delta x$ and the self inductance is $L\Delta x$ where R, L and C are per length variables.

If the conductor inside each slot is a wounded coil, then each wire is coupled to the neighboring wire by $K/\Delta x$. A slot with three turn coil and the corresponding couplings are graphically illustrated in Fig.7. It is important to mention that the overhangs model would have different values.

There have been a number of models introduced by some authors but they are mainly valid for transformer windings [9]-[12]. Since the geometry of transformers and electrical machines are different the transformer models cannot be necessarily applicable to machine windings. Nevertheless they give a good idea about the physics of wave propagation and the nature of differential equations which rules over the wave behavior.

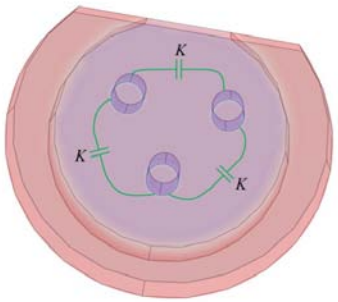

Fig. 7. Cross section of the slot slice with three wires inside, where each wire is coupled to its neighbor wire with capacitance K.

The R, L, C and K values inside the slot are different than the overhang. Nevertheless the equivalent high frequency circuit can be simplified to the model illustrated in Fig.8, where the R, L, C and K components of overhang and slot are combined and changed in a manner to fit into the repeated circuit of uniform sections over the whole winding. In the following, these equivalent uniform values will be derived.

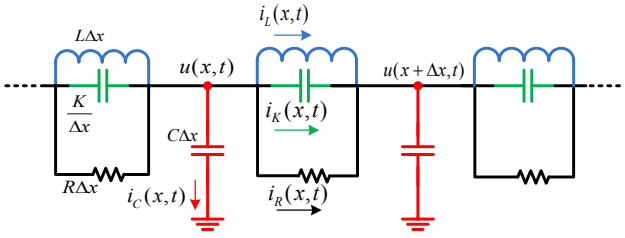

Fig. 8. Simplified high frequency model of machine winding.

Partial differential equation (4) describes the model of Fig.8 mathematically. More detailed calculations are presented in the Appendix.

$$\frac{1}{R}\frac{\partial^3 u(x,t)}{\partial x^2 \partial t} + K\frac{\partial^4 u(x,t)}{\partial x^2 \partial t^2} + \frac{1}{L}\frac{\partial^2 u(x,t)}{\partial x^2} = C\frac{\partial^2 u(x,t)}{\partial t^2} \qquad (7)$$

The constants described in (7)-(10) are notations used to describe the solution to the system of partial differential equation (7).

$$X_n = \frac{-4}{n\pi}\frac{\frac{C}{K}}{\lambda_n^2 + \frac{C}{K}} \quad \lambda_n = \left(\frac{n\pi}{2l}\right)^2, \quad n = 1,3,5,... \qquad (8)$$

$$\omega_n = \frac{\lambda_n}{\sqrt{L\left(C + \lambda_n^2 K\right)}} \qquad (9)$$

$$d_n = \frac{\lambda_n^2}{2R(C + \lambda_n^2 K)} \qquad (10)$$

By using the separation approach in solving partial differential equations, the voltage of the machine winding can be described by (11).

$$u(x,t) = 1 + \sum_n \Big(X_n \sin(\lambda_n x)\, e^{-d_n t} \left(\frac{d_n}{\omega_n}\sin\omega_n t + \cos\omega_n t\right) \Big) \qquad (11)$$

Equation (11) is a typical wave equation. Throughout the time, the oscillations travel back and forth inside the winding. For different values of *R*, *L*, *C* and *K*, the wave form looks different. The process to find the *R*, *L*, *C* and *K* values which fit the wave form the best is described step by step in the next section of this contribution.

V. Calculation of Parameters

The data from the measurement Case I and Case II can be interpolated and put into a computer model to extract the values of *R*, *L*, *C* and *K* in (11). The model follows the following rules:

A. Earth Capacitance-Coupling Capacitance

Knowing the geometry of wires and their distance towards each other, the capacitance *K* between two neighbor parallel wires is estimated from equation (12) according to [22]. In this equation, parameter D is the distance between two neighbor wires in a slot and *a* is the radius of the wire.

$$K \cong \frac{\pi \varepsilon_0 \varepsilon_r}{\mathrm{Ln}\left(\frac{D}{2a} + \sqrt{\left(\frac{D}{2a}\right)^2 - 1}\right)} \qquad (12)$$

The estimation of the voltage distribution is strongly influenced by the capacitive parameters *C* and *K*.

Knowing the measured oscillation frequency from both Case I and Case II, the value of *C* can be determined according to (13). Another method to derive the value of *C* is to use the initial voltage distribution formula described by Heller and Veverka [11].

$$\frac{\omega_{n\ \text{Case I}}}{\omega_{n\ \text{Case II}}} = \frac{\sqrt{1 + \frac{C}{K\lambda_{n\ \text{Case II}}^2}}}{\sqrt{1 + \frac{C}{K\lambda_{n\ \text{Case I}}^2}}} \qquad (13)$$

In the next section it will be discussed that the calculated and derived values are in compliance with the typical capacitive parameters of electrical machines [21]. These values are then used to determine the amplitude of each of the voltage space harmonics X_n in (8).

B. Oscillation Frequency

The period and frequency of the oscillation is determined from measurement. Knowing the value of *C* as well as *K*, the measured frequency is used to determine *L* by applying (9).

C. Maximum

The maximum value of the voltage at the end of the winding occurs at the first peak of the measured oscillating voltage. This is the first time, at which the time derivative of voltage in (11) is zero. This can help calculate, the d_n values in (10). Since all other factors are known, the *R* values can be determined.

VI. Simulation Results

Following the steps described in IV, the high frequency equivalent circuit was determined. The model converges, assuming the value of resistance is frequency dependant. This dependency is in compliance with previous studies concerning the high frequency losses induced inside the machine including the contribution of iron parts, e.g. of the magnetic circuit [23].

These values for the machine under test are calculated and the results are collected in Table. I.

TABLE I
PARAMETERS OF HIGH FREQUENCY EQUIVALENT CIRCUIT OF A SINGLE LAYER WOUND THREE PHASE SYNCHRONOUS MACHINE.

Parameter	Value	Description
R in Ω/m	0.0148 ω_n + 5323.3	Resistance as a function of angular frequency
L in mH/m	17.74	Inductance
C in pF/m	0.0518	Capacitance to earth
K in pF· m	70	Neighboring capacitance

The winding behavior is simulated when the terminal of phase U is connected to the source voltage and the voltage is then measured at the end of phase U of the winding. The results of the calculations by the mathematical model presented in (11) as well as laboratory measurements are plotted in Fig.9. It can be seen that the simulation results and measured voltage are in good agreement.

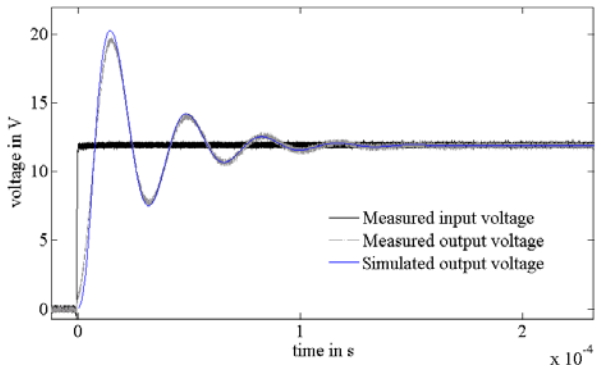

Fig. 9. A rectangular pulse with a 0.6 µs front is applied at the beginning of the phase U. The voltage at the end of the winding is measured and also simulated and the results are illustrated for comparison.

The calculated and simulated results for Case II, where the series connection of phase U and phase W are investigated, can be seen in Fig.10. It can be seen that they are in good agreement.

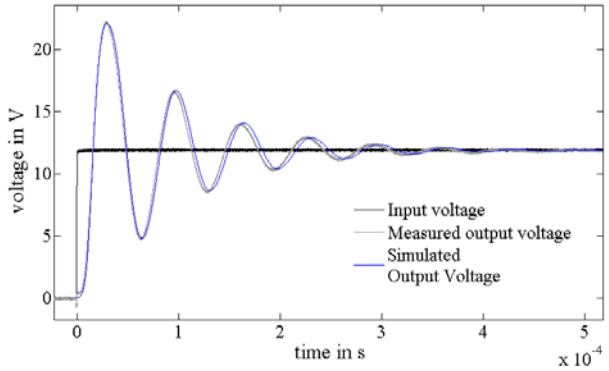

Fig. 10. A rectangular pulse with a 0.6µs front is applied at the beginning of series connection of phase U and V. The voltage at the end of the winding is then measured and also simulated and the results are illustrated for comparison.

Particular attention should be paid to the fact that the voltage is only measured at the beginning and end of the winding. From those measurements the high frequency parameters of the machine were derived.

VII. Distribution of Voltage Along the Winding

The derived parameters of *R*, *L*, *C* and *K* can be used to determine the voltage distribution along the entire winding being fed by a rectangular shaped voltage pulse. The simulation results are presented in Fig.11.

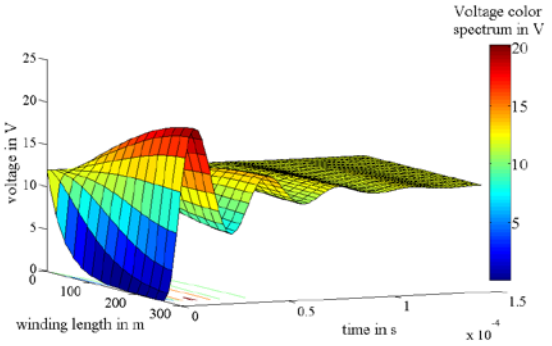

Fig. 11. Voltage distribution along the winding length of phase U with respect to time when a rectangular input voltage in connected to the machine terminal.

The results illustrate that due to the high frequency equivalent circuit, there exists a voltage increase equal to 1.68% of the imposed voltage. Furthermore, it can bee seen that the strongest voltage oscillations tend to dissipate after 0.1 ms.

VIII. Influence of Parameter on Machinery Transient and Lifetime

If the slot geometry, the magnetic circuit's geometry or its properties are changed, the quantities of the *R*, *L*, *C* and *K* will also change. As a consequence the constants in (11) and the distribution of voltage along the winding also change. Therefore, the voltage peaks may increase, which will increase the stress and reduce the expected life time of the machine. When changing the geometry of the slot, windings, iron parts or their material characteristics to optimize the power, torque, etc., it is important to investigate the voltage peaks and the time that voltage oscillations exert stress on the winding's insulation system. This approach can help make proper decisions about the choice of the insulation system to maintain the life time of electrical machines.

Fig.12 shows the simulation for the voltage distribution along the winding of phase U. The calculation was performed for the parameter *K* which is increased to 220 pF·m. It can be seen that the peak of the voltage is increased to 1.84% referred to the source voltage and that the winding still tends to oscillate even after 0.15 ms.

Another aspect that should be discussed here is the propagation speed as a function of the traveled distance. As observed and mentioned in part B of section III, when the travelled length of the wave is doubled by connecting two phases of the machine in series, the corresponding travelling time does not double. This is due to the existence of coupling capacitances that influences ω_n in (6). If the coupling factor *K* was equal to zero, the travelling time would be exactly proportional to the travelled length.

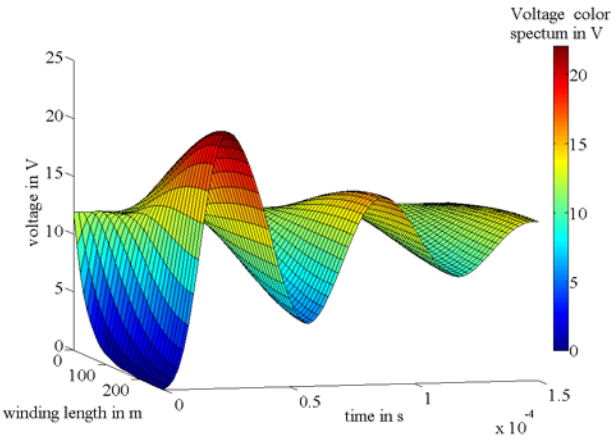

Fig. 12. Voltage distribution along the winding length of phase U with respect to time when a rectangular input voltage is connected to the machine terminal. In this simulation it is assumed that due to geometry changes K is increased to 220 pF·m.

IX. Conclusion

This paper is intended to describe a number of laboratory measurements to study the voltage wave propagation phenomenon in the winding of electrical

machines. Measurements have been performed at the terminals of the machine phases. The results validate that the application of a high frequency model for the analysis of inverter fed machines is necessary. Addressing the physical basis governing this phenomenon, a well studied high frequency model was introduced and its parameters were then derived from the measured voltage waveforms. When the machine voltage has a high harmonic frequency content due to inverter impulses, this model can simulate the behavior of the electrical machine winding. Observations of the winding oscillations and voltage peaks explain the reason why inverter fed machines tend to age faster and have a shorter life time expectation.

The derived model can be applied to analyze the propagation of fault signals like partial discharge and bearing currents in new and aged windings. The validity of this method on different machine types is not investigated yet. This will be the topic of the ongoing research.

X. APPENDIX

For the elements in Fig.8, the following Voltage and current equations are valid:

$$R\Delta x\, i_R(x,t) = u(x,t) - u(x+\Delta x,t) \tag{14}$$

$$L\Delta x \frac{di_L(x,t)}{dt} = u(x,t) - u(x+\Delta x,t) \tag{15}$$

$$i_K(x,t) = \frac{K}{\Delta x}\frac{d}{dt}\left(u(x,t) - u(x+\Delta x,t)\right) \tag{16}$$

$$i_C(x,t) = C\Delta x \frac{du(x+\Delta x,t)}{dt} \tag{17}$$

Combining the last four equations, the partial differential equation describing the voltage can be derived as in (7).

XI. REFERENCES

[1] J. Kaufhold, Kaufhold, " Evaluation Analysis of Thermal Ageing in Insulation Systems of Electrical Machine- A Historical Review -," *IEEE Trans. Power Delivery*, vol. 17, pp. 1373-1377, Oct. 2007.

[2] E. L. Brancato, "Insulation Aging, A Historical and Critical Review," *IEEE Trans. Electrical Insulation*, vol. EI-13, No 4, Aug. 1987.

[3] V.M. Montsinger, "Loading Transformers by temperature," *AIEETrans*. vol. 49, pp. 776-790, 1930.

[4] N. Hayakawa, H. Inano, K. Inuzuka, M. Morikawa, H. Okubo, "Partial Discharge Propagation and Degradation Characteristics of Magnet Wire for Inverter-Fed Motor under Surge Voltage Application," *IEEE Conf. Electrical Insulation and Dielectric Phenomena,* pp. 565-568, Oct 2006.

[5] L. A. Saunders, G. L. Skibinski, S. T. Evon, D.L. Kempkes, " Riding the reflected wave-IGBT drive technology demands new motor and cable considerations -IGBT drive technology demands new motor and cable considerations", *Proc. IEEE PCIC Conf.*, Philadelphia, PA, pp. 75–84, Sep. 1996.

[6] Melfi, M.J., "Low-Voltage PWM inverter-fed motor insulation issues", *IEEE Trans. Industry Applications,* vol. 42, Issue: 1, pp. 128 - 133, Jan.-Feb. 2006.

[7] J Erdman, R. J. Kerkman, D. Schlegel, G. Skibinski, "Effect of PWM Inverters on AC Motor Bearing Currents and Shaft Voltages," *IEEE Trans. Industry Applicatiopns*, Vol.32, No. 2, Mar. -Apr. 1996.

[8] "IEEE Trial-Use Guide to the Measurement of Partial Discharges in Rotating Machinery", *IEEE Std 1434-2000*, April 2000

[9] R. Rüdenberg, "Performance of traveling waves in coils and windings", *Trans. AIEE*, vol. 59, pp. 1031–1040, 1940.

[10] P. A. Abetti , G. E. Adams, F. J. Maginniss, "Oscillations of Coupled Windings", *Trans. AIEE*, pp. 12–21, Apr. 1955.

[11] B. Heller, A. Veverka, " Surge Voltages in Electrical Machines" VEB Verlag Technik Berlin, 1957.

[12] F. D. Torre, A. P. Morando, G. Todeschini, " Three-Phase Distributed Model of High-Voltage Windings to Study Internal Steep-Fronted Surge Propagation in a Straightforward Transformer", *IEEE Trans. Power Delivery*, vol. 23, NO. 4, Oct. 2008.

[13] S. Islam, G. Ledwich, "An Equivalent Circuit for Calculation of Interturn Voltage Distribution of Stator Windings in the Presence of Slot Discharges", Proc. of the 5th International Conf. on Properties and Applications of Dielectric Materials, May 1997.

[14] "Bearing currents in modern AC drive systems", ABB drives, Technical guide No. 5

[15] "Induction motors fed by PWM frequency inverters", WEG Technical guide

[16] R. Belmans, D. Verdyck, W. Geysen, and R. Findlay, "Electromechanical Analysis of the Audible Noise of an Inverter-fed Squirrel-cage Induction Motor," IEEE Trans. Ind. Appl., vol. 27, No. 3, pp. 539–544, May.-Jun. 1991.

[17] A. Wilson, R. J. Jackson, N. Wang, "Discharge Detection Techniques for Stator Windings", *IEE Proceedings B in Electric Power Applications,* vol. 132, Issue: 5, September 1985.

[18] A.Obralic, "Winding Diagnose on Rotating Electrical Machines with the help of Digital Synchronous Multichannel PD analysis", Ph.D. dissertation, Faculty of Elektrotechnik und Informatik, TU Berlin, 2008.

[19] D. Cheng, "Field and Wave Electromagnetics", ADDISON WESLEY, 1989.

[20] P. J. Tavner, R. J. Jackson, "Coupling of Discharge Currents between Conductors of Electrical Machines owing to Laminated Steel Core", *IEE Proc. B Elec. Power Applications*, vol.135, Issue:6, pp 295-307, Nov. 2008.

[21] T. Humiston, P. Pillay, "Parameter measurements to study surge propagation in induction machines," *IEEE Trans. Ind. Appl*., vol. 40, no. 5, pp. 1341–1348, Sep.- Oct. 2004.

[22] H. E. Green, "A simplified derivation of the capacitance of a two wire line", *IEEE Trans. Microwave Theory Tech*., Vol. 47, no. 3, pp.365–366, Mar. 1999.

[23] H. Bondi, K. C. Mukherji, "An Analysis of Tooth-Ripple Phenomena in Smooth Laminated Pole-Shoes", *Proc. IEE - Part C: Monographs*, vol.104, Issue: 6, pp. 349 – 356, Sep. 1957.

XII. BIOGRAPHIES

Sara Mahdavi finished her B.Sc in electrical power engineering at Tehran University, Tehran. Iran. She received her Master degree in the same subject from the Technical University of Darmstadt, Darmstadt, Germany.

She has been employed by the electricity distribution company, Tehran, Iran. She also has worked in the Energy Research Center, Tehran, Iran.

She has been working as a research associate at the Institute of Electrical Machines of RWTH Aachen University, Germany since May 2011.

Her research interests include transient and high frequency modeling of electrical machines and condition monitoring tests.

Kay Hameyer (M'96-SM'99) received the M.Sc. degree in electrical engineering from the University of Hannover, Hannover, Germany, and the Ph.D. degree from the University of Technology Berlin, Berlin, Germany.

After his university studies, he was with Robert Bosch GmbH, Stuttgart, Germany, as a Design Engineer for permanent-magnet servo motors and electrical board net components for vehicles.

Until February 2004, he was a Full Professor of numerical field computations and electrical machines at the Katholieke Universiteit Leuven, Belgium,. Since 2004 he is currently a Full Professor, the Director of the Institute of Electrical Machines, and the holder of the Chair Electromagnetic Energy Conversion at RWTH Aachen University, Aachen, Germany, where he has been the Dean of the Faculty of Electrical Engineering and Information Technology from 2007 to2009.

His research interests include numerical field computation and simulation, design of electrical machines, particularly permanent-magnet excited machines and induction machines, and numerical optimization strategies.